Search for the rare decay $B_s^0 \to \phi\mu^+\mu^-$ with the D0 detector

V. M. Abazov,[36] B. Abbott,[76] M. Abolins,[66] B. S. Acharya,[29] M. Adams,[52] T. Adams,[50] M. Agelou,[18] J.-L. Agram,[19] S. H. Ahn,[31] M. Ahsan,[60] G. D. Alexeev,[36] G. Alkhazov,[40] A. Alton,[65] G. Alverson,[64] G. A. Alves,[2] M. Anastasoaie,[35] T. Andeen,[54] S. Anderson,[46] B. Andrieu,[17] M. S. Anzelc,[54] Y. Arnoud,[14] M. Arov,[53] A. Askew,[50] B. Åsman,[41] A. C. S. Assis Jesus,[3] O. Atramentov,[58] C. Autermann,[21] C. Avila,[8] C. Ay,[24] F. Badaud,[13] A. Baden,[62] L. Bagby,[53] B. Baldin,[51] D. V. Bandurin,[36] P. Banerjee,[29] S. Banerjee,[29] E. Barberis,[64] P. Bargassa,[81] P. Baringer,[59] C. Barnes,[44] J. Barreto,[2] J. F. Bartlett,[51] U. Bassler,[17] D. Bauer,[44] A. Bean,[59] M. Begalli,[3] M. Begel,[72] C. Belanger-Champagne,[5] A. Bellavance,[68] J. A. Benitez,[66] S. B. Beri,[27] G. Bernardi,[17] R. Bernhard,[42] L. Berntzon,[15] I. Bertram,[43] M. Besançon,[18] R. Beuselinck,[44] V. A. Bezzubov,[39] P. C. Bhat,[51] V. Bhatnagar,[27] M. Binder,[25] C. Biscarat,[43] K. M. Black,[63] I. Blackler,[44] G. Blazey,[53] F. Blekman,[44] S. Blessing,[50] D. Bloch,[19] K. Bloom,[68] U. Blumenschein,[23] A. Boehnlein,[51] O. Boeriu,[56] T. A. Bolton,[60] F. Borcherding,[51] G. Borissov,[43] K. Bos,[34] T. Bose,[78] A. Brandt,[79] R. Brock,[66] G. Brooijmans,[71] A. Bross,[51] D. Brown,[79] N. J. Buchanan,[50] D. Buchholz,[54] M. Buehler,[82] V. Buescher,[23] S. Burdin,[51] S. Burke,[46] T. H. Burnett,[83] E. Busato,[17] C. P. Buszello,[44] J. M. Butler,[63] S. Calvet,[15] J. Cammin,[72] S. Caron,[34] W. Carvalho,[3] B. C. K. Casey,[78] N. M. Cason,[56] H. Castilla-Valdez,[33] S. Chakrabarti,[29] D. Chakraborty,[53] K. M. Chan,[72] A. Chandra,[49] D. Chapin,[78] F. Charles,[19] E. Cheu,[46] F. Chevallier,[14] D. K. Cho,[63] S. Choi,[32] B. Choudhary,[28] L. Christofek,[59] D. Claes,[68] B. Clément,[19] C. Clément,[41] Y. Coadou,[5] J. Coenen,[21] M. Cooke,[81] W. E. Cooper,[51] D. Coppage,[59] M. Corcoran,[81] M.-C. Cousinou,[15] B. Cox,[45] S. Crépé-Renaudin,[14] D. Cutts,[78] M. Ćwiok,[30] H. da Motta,[2] A. Das,[63] M. Das,[61] B. Davies,[43] G. Davies,[44] G. A. Davis,[54] K. De,[79] P. de Jong,[34] S. J. de Jong,[35] E. De La Cruz-Burelo,[65] C. De Oliveira Martins,[3] J. D. Degenhardt,[65] F. Déliot,[18] M. Demarteau,[51] R. Demina,[72] P. Demine,[18] D. Denisov,[51] S. P. Denisov,[39] S. Desai,[73] H. T. Diehl,[51] M. Diesburg,[51] M. Doidge,[43] A. Dominguez,[68] H. Dong,[73] L. V. Dudko,[38] L. Duflot,[16] S. R. Dugad,[29] A. Duperrin,[15] J. Dyer,[66] A. Dyshkant,[53] M. Eads,[68] D. Edmunds,[66] T. Edwards,[45] J. Ellison,[49] J. Elmsheuser,[25] V. D. Elvira,[51] S. Eno,[62] P. Ermolov,[38] J. Estrada,[51] H. Evans,[55] A. Evdokimov,[37] V. N. Evdokimov,[39] S. N. Fatakia,[63] L. Feligioni,[63] A. V. Ferapontov,[60] T. Ferbel,[72] F. Fiedler,[25] F. Filthaut,[35] W. Fisher,[51] H. E. Fisk,[51] I. Fleck,[23] M. Ford,[45] M. Fortner,[53] H. Fox,[23] S. Fu,[51] S. Fuess,[51] T. Gadfort,[83] C. F. Galea,[35] E. Gallas,[51] E. Galyaev,[56] C. Garcia,[72] A. Garcia-Bellido,[83] J. Gardner,[59] V. Gavrilov,[37] A. Gay,[19] P. Gay,[13] D. Gelé,[19] R. Gelhaus,[49] C. E. Gerber,[52] Y. Gershtein,[50] D. Gillberg,[5] G. Ginther,[72] N. Gollub,[41] B. Gómez,[8] K. Gounder,[51] A. Goussiou,[56] P. D. Grannis,[73] H. Greenlee,[51] Z. D. Greenwood,[61] E. M. Gregores,[4] G. Grenier,[20] Ph. Gris,[13] J.-F. Grivaz,[16] S. Grünendahl,[51] M. W. Grünewald,[30] F. Guo,[73] J. Guo,[73] G. Gutierrez,[51] P. Gutierrez,[76] A. Haas,[71] N. J. Hadley,[62] P. Haefner,[25] S. Hagopian,[50] J. Haley,[69] I. Hall,[76] R. E. Hall,[48] L. Han,[7] K. Hanagaki,[51] K. Harder,[60] A. Harel,[72] R. Harrington,[64] J. M. Hauptman,[58] R. Hauser,[66] J. Hays,[54] T. Hebbeker,[21] D. Hedin,[53] J. G. Hegeman,[34] J. M. Heinmiller,[52] A. P. Heinson,[49] U. Heintz,[63] C. Hensel,[59] G. Hesketh,[64] M. D. Hildreth,[56] R. Hirosky,[82] J. D. Hobbs,[73] B. Hoeneisen,[12] M. Hohlfeld,[16] S. J. Hong,[31] R. Hooper,[78] P. Houben,[34] Y. Hu,[73] V. Hynek,[9] I. Iashvili,[70] R. Illingworth,[51] A. S. Ito,[51] S. Jabeen,[63] M. Jaffré,[16] S. Jain,[76] K. Jakobs,[23] C. Jarvis,[62] A. Jenkins,[44] R. Jesik,[44] K. Johns,[46] C. Johnson,[71] M. Johnson,[51] A. Jonckheere,[51] P. Jonsson,[44] A. Juste,[51] D. Käfer,[21] S. Kahn,[74] E. Kajfasz,[15] A. M. Kalinin,[36] J. M. Kalk,[61] J. R. Kalk,[66] S. Kappler,[21] D. Karmanov,[38] J. Kasper,[63] I. Katsanos,[71] D. Kau,[50] R. Kaur,[27] R. Kehoe,[80] S. Kermiche,[15] S. Kesisoglou,[78] A. Khanov,[77] A. Kharchilava,[70] Y. M. Kharzheev,[36] D. Khatidze,[71] H. Kim,[79] T. J. Kim,[31] M. H. Kirby,[35] B. Klima,[51] J. M. Kohli,[27] J.-P. Konrath,[23] M. Kopal,[76] V. M. Korablev,[39] J. Kotcher,[74] B. Kothari,[71] A. Koubarovsky,[38] A. V. Kozelov,[39] J. Kozminski,[66] A. Kryemadhi,[82] S. Krzywdzinski,[51] T. Kuhl,[24] A. Kumar,[70] S. Kunori,[62] A. Kupco,[11] T. Kurča,[20,*] J. Kvita,[9] S. Lager,[41] S. Lammers,[71] G. Landsberg,[78] J. Lazoflores,[50] A.-C. Le Bihan,[19] P. Lebrun,[20] W. M. Lee,[53] A. Leflat,[38] F. Lehner,[42] C. Leonidopoulos,[71] V. Lesne,[13] J. Leveque,[46] P. Lewis,[44] J. Li,[79] Q. Z. Li,[51] J. G. R. Lima,[53] D. Lincoln,[51] J. Linnemann,[66] V. V. Lipaev,[39] R. Lipton,[51] Z. Liu,[5] L. Lobo,[44] A. Lobodenko,[40] M. Lokajicek,[11] A. Lounis,[19] P. Love,[43] H. J. Lubatti,[83] M. Lynker,[56] A. L. Lyon,[51] A. K. A. Maciel,[2] R. J. Madaras,[47] P. Mättig,[26] C. Magass,[21] A. Magerkurth,[65] A.-M. Magnan,[14] N. Makovec,[16] P. K. Mal,[56] H. B. Malbouisson,[3] S. Malik,[68] V. L. Malyshev,[36] H. S. Mao,[6] Y. Maravin,[60] M. Martens,[51] S. E. K. Mattingly,[78] R. McCarthy,[73] R. McCroskey,[46] D. Meder,[24] A. Melnitchouk,[67] A. Mendes,[15] L. Mendoza,[8] M. Merkin,[38] K. W. Merritt,[51] A. Meyer,[21] J. Meyer,[22] M. Michaut,[18] H. Miettinen,[81] T. Millet,[20] J. Mitrevski,[71] J. Molina,[3] N. K. Mondal,[29] J. Monk,[45] R. W. Moore,[5] T. Moulik,[59] G. S. Muanza,[16] M. Mulders,[51] M. Mulhearn,[71] L. Mundim,[3] Y. D. Mutaf,[73] E. Nagy,[15] M. Naimuddin,[28] M. Narain,[63] N. A. Naumann,[35] H. A. Neal,[65] J. P. Negret,[8] S. Nelson,[50] P. Neustroev,[40] C. Noeding,[23] A. Nomerotski,[51] S. F. Novaes,[4] T. Nunnemann,[25] V. O'Dell,[51] D. C. O'Neil,[5] G. Obrant,[40] V. Oguri,[3] N. Oliveira,[3] N. Oshima,[51] R. Otec,[10] G. J. Otero y Garzón,[52] M. Owen,[45] P. Padley,[81] N. Parashar,[57] S.-J. Park,[72] S. K. Park,[31] J. Parsons,[71] R. Partridge,[78] N. Parua,[73] A. Patwa,[74] G. Pawloski,[81] P. M. Perea,[49] E. Perez,[18] K. Peters,[45]

P. Pétroff,[16] M. Petteni,[44] R. Piegaia,[1] M.-A. Pleier,[22] P. L. M. Podesta-Lerma,[33] V. M. Podstavkov,[51] Y. Pogorelov,[56] M.-E. Pol,[2] A. Pompoš,[76] B. G. Pope,[66] A. V. Popov,[39] W. L. Prado da Silva,[3] H. B. Prosper,[50] S. Protopopescu,[74] J. Qian,[65] A. Quadt,[22] B. Quinn,[67] K. J. Rani,[29] K. Ranjan,[28] P. A. Rapidis,[51] P. N. Ratoff,[43] P. Renkel,[80] S. Reucroft,[64] M. Rijssenbeek,[73] I. Ripp-Baudot,[19] F. Rizatdinova,[77] S. Robinson,[44] R. F. Rodrigues,[3] C. Royon,[18] P. Rubinov,[51] R. Ruchti,[56] V. I. Rud,[38] G. Sajot,[14] A. Sánchez-Hernández,[33] M. P. Sanders,[62] A. Santoro,[3] G. Savage,[51] L. Sawyer,[61] T. Scanlon,[44] D. Schaile,[25] R. D. Schamberger,[73] Y. Scheglov,[40] H. Schellman,[54] P. Schieferdecker,[25] C. Schmitt,[26] C. Schwanenberger,[45] A. Schwartzman,[69] R. Schwienhorst,[66] S. Sengupta,[50] H. Severini,[76] E. Shabalina,[52] M. Shamim,[60] V. Shary,[18] A. A. Shchukin,[39] W. D. Shephard,[56] R. K. Shivpuri,[28] D. Shpakov,[64] V. Siccardi,[19] R. A. Sidwell,[60] V. Simak,[10] V. Sirotenko,[51] P. Skubic,[76] P. Slattery,[72] R. P. Smith,[51] G. R. Snow,[68] J. Snow,[75] S. Snyder,[74] S. Söldner-Rembold,[45] X. Song,[53] L. Sonnenschein,[17] A. Sopczak,[43] M. Sosebee,[79] K. Soustruznik,[9] M. Souza,[2] B. Spurlock,[79] J. Stark,[14] J. Steele,[61] K. Stevenson,[55] V. Stolin,[37] A. Stone,[52] D. A. Stoyanova,[39] J. Strandberg,[41] M. A. Strang,[70] M. Strauss,[76] R. Ströhmer,[25] D. Strom,[54] M. Strovink,[47] L. Stutte,[51] S. Sumowidagdo,[50] A. Sznajder,[3] M. Talby,[15] P. Tamburello,[46] W. Taylor,[5] P. Telford,[45] J. Temple,[46] B. Tiller,[25] M. Titov,[23] V. V. Tokmenin,[36] M. Tomoto,[51] T. Toole,[62] I. Torchiani,[23] S. Towers,[43] T. Trefzger,[24] S. Trincaz-Duvoid,[17] D. Tsybychev,[73] B. Tuchming,[18] C. Tully,[69] A. S. Turcot,[45] P. M. Tuts,[71] R. Unalan,[66] L. Uvarov,[40] S. Uvarov,[40] S. Uzunyan,[53] B. Vachon,[5] P. J. van den Berg,[34] R. Van Kooten,[55] W. M. van Leeuwen,[34] N. Varelas,[52] E. W. Varnes,[46] A. Vartapetian,[79] I. A. Vasilyev,[39] M. Vaupel,[26] P. Verdier,[20] L. S. Vertogradov,[36] M. Verzocchi,[51] F. Villeneuve-Seguier,[44] P. Vint,[44] J.-R. Vlimant,[17] E. Von Toerne,[60] M. Voutilainen,[68,†] M. Vreeswijk,[34] H. D. Wahl,[50] L. Wang,[62] J. Warchol,[56] G. Watts,[83] M. Wayne,[56] M. Weber,[51] H. Weerts,[66] N. Wermes,[22] M. Wetstein,[62] A. White,[79] D. Wicke,[26] G. W. Wilson,[59] S. J. Wimpenny,[49] M. Wobisch,[51] J. Womersley,[51] D. R. Wood,[64] T. R. Wyatt,[45] Y. Xie,[78] N. Xuan,[56] S. Yacoob,[54] R. Yamada,[51] M. Yan,[62] T. Yasuda,[51] Y. A. Yatsunenko,[36] K. Yip,[74] H. D. Yoo,[78] S. W. Youn,[54] C. Yu,[14] J. Yu,[79] A. Yurkewicz,[73] A. Zatserklyaniy,[53] C. Zeitnitz,[26] D. Zhang,[51] T. Zhao,[83] Z. Zhao,[65] B. Zhou,[65] J. Zhu,[73] M. Zielinski,[72] D. Zieminska,[55] A. Zieminski,[55] V. Zutshi,[53] and E. G. Zverev[38]

(D0 Collaboration)

[1]*Universidad de Buenos Aires, Buenos Aires, Argentina*
[2]*LAFEX, Centro Brasileiro de Pesquisas Físicas, Rio de Janeiro, Brazil*
[3]*Universidade do Estado do Rio de Janeiro, Rio de Janeiro, Brazil*
[4]*Instituto de Física Teórica, Universidade Estadual Paulista, São Paulo, Brazil*
[5]*University of Alberta, Edmonton, Alberta, Canada, Simon Fraser University, Burnaby, British Columbia, Canada, York University, Toronto, Ontario, Canada, and McGill University, Montreal, Quebec, Canada*
[6]*Institute of High Energy Physics, Beijing, People's Republic of China*
[7]*University of Science and Technology of China, Hefei, People's Republic of China*
[8]*Universidad de los Andes, Bogotá, Colombia*
[9]*Center for Particle Physics, Charles University, Prague, Czech Republic*
[10]*Czech Technical University, Prague, Czech Republic*
[11]*Center for Particle Physics, Institute of Physics, Academy of Sciences of the Czech Republic, Prague, Czech Republic*
[12]*Universidad San Francisco de Quito, Quito, Ecuador*
[13]*Laboratoire de Physique Corpusculaire, IN2P3-CNRS, Université Blaise Pascal, Clermont-Ferrand, France*
[14]*Laboratoire de Physique Subatomique et de Cosmologie, IN2P3-CNRS, Universite de Grenoble 1, Grenoble, France*
[15]*CPPM, IN2P3-CNRS, Université de la Méditerranée, Marseille, France*
[16]*IN2P3-CNRS, Laboratoire de l'Accélérateur Linéaire, Orsay, France*
[17]*LPNHE, IN2P3-CNRS, Universités Paris VI and VII, Paris, France*
[18]*DAPNIA/Service de Physique des Particules, CEA, Saclay, France*
[19]*IReS, IN2P3-CNRS, Université Louis Pasteur, Strasbourg, France, and Université de Haute Alsace, Mulhouse, France*
[20]*Institut de Physique Nucléaire de Lyon, IN2P3-CNRS, Université Claude Bernard, Villeurbanne, France*
[21]*III. Physikalisches Institut A, RWTH Aachen, Aachen, Germany*
[22]*Physikalisches Institut, Universität Bonn, Bonn, Germany*
[23]*Physikalisches Institut, Universität Freiburg, Freiburg, Germany*
[24]*Institut für Physik, Universität Mainz, Mainz, Germany*
[25]*Ludwig-Maximilians-Universität München, München, Germany*
[26]*Fachbereich Physik, University of Wuppertal, Wuppertal, Germany*
[27]*Panjab University, Chandigarh, India*
[28]*Delhi University, Delhi, India*
[29]*Tata Institute of Fundamental Research, Mumbai, India*

[30]University College Dublin, Dublin, Ireland

[31]Korea Detector Laboratory, Korea University, Seoul, Korea

[32]SungKyunKwan University, Suwon, Korea

[33]CINVESTAV, Mexico City, Mexico

[34]FOM-Institute NIKHEF and University of Amsterdam/NIKHEF, Amsterdam, The Netherlands

[35]Radboud University Nijmegen/NIKHEF, Nijmegen, The Netherlands

[36]Joint Institute for Nuclear Research, Dubna, Russia

[37]Institute for Theoretical and Experimental Physics, Moscow, Russia

[38]Moscow State University, Moscow, Russia

[39]Institute for High Energy Physics, Protvino, Russia

[40]Petersburg Nuclear Physics Institute, St. Petersburg, Russia

[41]Lund University, Lund, Sweden, Royal Institute of Technology
and Stockholm University, Stockholm, Sweden, and Uppsala University, Uppsala, Sweden

[42]Physik Institut der Universität Zürich, Zürich, Switzerland

[43]Lancaster University, Lancaster, United Kingdom

[44]Imperial College, London, United Kingdom

[45]University of Manchester, Manchester, United Kingdom

[46]University of Arizona, Tucson, Arizona 85721, USA

[47]Lawrence Berkeley National Laboratory
and University of California, Berkeley, California 94720, USA

[48]California State University, Fresno, California 93740, USA

[49]University of California, Riverside, California 92521, USA

[50]Florida State University, Tallahassee, Florida 32306, USA

[51]Fermi National Accelerator Laboratory, Batavia, Illinois 60510, USA

[52]University of Illinois at Chicago, Chicago, Illinois 60607, USA

[53]Northern Illinois University, DeKalb, Illinois 60115, USA

[54]Northwestern University, Evanston, Illinois 60208, USA

[55]Indiana University, Bloomington, Indiana 47405, USA

[56]University of Notre Dame, Notre Dame, Indiana 46556, USA

[57]Purdue University Calumet, Hammond, Indiana 46323, USA

[58]Iowa State University, Ames, Iowa 50011, USA

[59]University of Kansas, Lawrence, Kansas 66045, USA

[60]Kansas State University, Manhattan, Kansas 66506, USA

[61]Louisiana Tech University, Ruston, Louisiana 71272, USA

[62]University of Maryland, College Park, Maryland 20742, USA

[63]Boston University, Boston, Massachusetts 02215, USA

[64]Northeastern University, Boston, Massachusetts 02115, USA

[65]University of Michigan, Ann Arbor, Michigan 48109, USA

[66]Michigan State University, East Lansing, Michigan 48824, USA

[67]University of Mississippi, University, Mississippi 38677, USA

[68]University of Nebraska, Lincoln, Nebraska 68588, USA

[69]Princeton University, Princeton, New Jersey 08544, USA

[70]State University of New York, Buffalo, New York 14260, USA

[71]Columbia University, New York, New York 10027, USA

[72]University of Rochester, Rochester, New York 14627, USA

[73]State University of New York, Stony Brook, New York 11794, USA

[74]Brookhaven National Laboratory, Upton, New York 11973, USA

[75]Langston University, Langston, Oklahoma 73050, USA

[76]University of Oklahoma, Norman, Oklahoma 73019, USA

[77]Oklahoma State University, Stillwater, Oklahoma 74078, USA

[78]Brown University, Providence, Rhode Island 02912, USA

[79]University of Texas, Arlington, Texas 76019, USA

[80]Southern Methodist University, Dallas, Texas 75275, USA

[81]Rice University, Houston, Texas 77005, USA

[82]University of Virginia, Charlottesville, Virginia 22901, USA

[83]University of Washington, Seattle, Washington 98195, USA

*On leave from IEP SAS Kosice, Slovakia.

†Visitor from Helsinki Institute of Physics, Helsinki, Finland.

We present a search for the flavor-changing neutral current decay $B_s^0 \to \phi \mu^+ \mu^-$ using about 0.45 fb^{-1} of data collected in $p\bar{p}$ collisions at $\sqrt{s} = 1.96$ TeV with the D0 detector at the Fermilab Tevatron Collider. We find an upper limit on the branching ratio of this decay normalized to $B_s^0 \to J/\psi\phi$ of $\frac{\mathcal{B}(B_s^0 \to \phi\mu^+\mu^-)}{\mathcal{B}(B_s^0 \to J/\psi\phi)} < 4.4 \times 10^{-3}$ at the 95% C.L. Using the central value of the world average branching fraction of $B_s^0 \to J/\psi\phi$, the limit corresponds to $\mathcal{B}(B_s^0 \to \phi\mu^+\mu^-) < 4.1 \times 10^{-6}$ at the 95% C.L., the most stringent upper bound to date.

The investigation of rare flavor-changing neutral current (FCNC) B meson decays has received special attention in the past since this opens up the possibility of precision tests of the flavor structure of the standard model (SM). In the SM, FCNC decays are absent at tree level but proceed at higher order through electroweak penguin and box diagrams. FCNC decays are sensitive to new physics, since decay amplitudes involving new particles interfere with SM amplitudes. Although inclusive FCNC decays like $B \to X_s \ell^+ \ell^-$ or $B \to X_s \gamma$ are theoretically easier to calculate, exclusive decays with one hadron in the final state are experimentally easier to study. For instance, the exclusive decays $B_d^0 \to K^* \ell^+ \ell^-$ and $B^\pm \to K^\pm \ell^+ \ell^-$ have been already measured at B-factories [1,2] and were found to be consistent with the SM within the present experimental uncertainties. Related to the same quark-level transition of $b \to s \ell^+ \ell^-$ is the corresponding exclusive FCNC decay $B_s^0 \to \phi \mu^+ \mu^-$ in the B_s^0 meson system. An observation of this decay or experimental upper limit on its rate will yield additional important information on the flavor dynamics of FCNC decays.

Within the SM, the decay rate for the $B_s^0 \to \phi \mu^+ \mu^-$ decay, neglecting the interference effects with the much stronger $B_s^0 \to J/\psi\phi$ and $B_s^0 \to \psi(2S)\phi$ resonance decays, is predicted to be of the order of 1.6×10^{-6} [3] with about 30% uncertainty due to poorly known form factors. The interference effects with the B_s^0 resonance decay amplitudes are large, with their expected magnitude depending on the exact modeling of the charmonium states [4]. To separate experimentally the FCNC-mediated process $B_s^0 \to \phi \mu^+ \mu^-$, one has to restrict the invariant mass of the final state lepton pair to be outside the charmonium resonances. Presently, the only existing experimental bound on the $B_s^0 \to \phi \mu^+ \mu^-$ decay is given by CDF from the analysis of Run I data [5]. CDF sets an upper limit at the 95% C.L. of $\mathcal{B}(B_s^0 \to \phi \mu^+ \mu^-) < 6.7 \times 10^{-5}$.

In this Letter, we report on a new experimental limit of the decay $B_s^0 \to \phi \mu^+ \mu^-$, that is an order of magnitude more stringent than the existing limit. The ϕ mesons are reconstructed through their $K^+ K^-$ decay mode assuming the two tracks forming the ϕ candidate to be kaons. The invariant mass of the two muons in the final state is required to be outside the charmonium resonances. The events in our search are normalized to resonant decay $B_s^0 \to J/\psi\phi$ events. Using the $B_s^0 \to J/\psi\phi$ mode as the

normalization channel has the advantage that the efficiencies to detect the $\phi \mu^+ \mu^-$ system in signal and normalization events are similar, and systematic effects tend to cancel.

The search uses a data set corresponding to approximately 0.45 fb^{-1} of $p\bar{p}$ collisions at $\sqrt{s} = 1.96$ TeV recorded by the D0 detector operating at the Fermilab Tevatron Collider. The D0 detector is described in detail elsewhere [6]. The main elements relevant for this analysis are the central tracking and muon detector systems. The central tracking system consists of a silicon microstrip tracker (SMT) and a central fiber tracker (CFT), both located within a 2 T superconducting solenoidal magnet. The muon detector, which is located outside the calorimeter, consists of a layer of tracking detectors and scintillation trigger counters in front of 1.8 T toroidal magnets, followed by two more similar layers after the toroids, allowing for efficient muon detection out to pseudorapidity (η) of ± 2.2.

Dimuon triggers were used in the data selection for this analysis. A trigger simulation was used to estimate the trigger efficiency for the signal and normalization samples. These efficiencies were also checked with samples of J/ψ events collected with single muon triggers [7]. The trigger is almost fully efficient for muons above 5 GeV/c already at the first level.

The event preselection starts with a loose selection of $B_s^0 \to \phi \mu^+ \mu^-$ candidates. These candidates are identified by requiring exactly two muons fulfilling quality cuts on the number of hits in the muon system and the two additional charged particle tracks to form a good vertex. The reconstructed invariant mass of the B_s^0 candidate should be within $4.4 < m_{\phi\mu^+\mu^-} < 6.2$ GeV/c^2.

We then require the invariant mass of the two muons to be within $0.5 < m_{\mu^+\mu^-} < 4.4$ GeV/c^2. In this mass region, the $J/\psi(\to \mu^+ \mu^-)$ and $\psi(2S)(\to \mu^+ \mu^-)$ resonances are excluded to discriminate against dominant resonant decays by rejecting the mass region $2.72 < m_{\mu^+\mu^-} < 4.06$ GeV/c^2. The J/ψ mass resolution in data is given by a Gaussian distribution with $\sigma = 75$ MeV/c^2. The rejected mass region then covers $\pm 5\sigma$ wide windows around the resonance masses.

The χ^2/d.o.f. of the two-muon vertex is required to be less than 10. The tracks that are matched to each muon are

TABLE I. Number of candidate events surviving the cuts in data used in the preselection analysis.

Selection criteria	Value	# candidates
Good B_s^0 vertex		1555320
Mass region (GeV/c^2)	$0.5 < m_{\mu^+\mu^-} < 4.4$ excl. $J/\psi, \psi(2S)$	530892
Muon quality		276875
χ^2/d.o.f. of vertex	<10	127509
Muon p_T (GeV/c)	>2.5	73555
Muon $|\eta|$	<2.0	72350
Tracking hits	CFT > 3, SMT > 2	58012
δL_{xy} (mm)	<0.15	54752
B_s^0 candidate p_T (GeV/c)	>5.0	54399
$B_s^0 \chi^2$ vertex	<36	53195
Kaon p_T (GeV/c)	>0.7	9639
ϕ mass (GeV/c^2)	$1.008 < m_\phi < 1.032$	2602

required to have at least three (four) measurements in the SMT (CFT) and the transverse momentum of each of the muons (p_T^μ) is required to be greater than 2.5 GeV/c with $|\eta| < 2.0$ to be well inside the fiducial tracking and muon detector acceptances. In order to select well-measured secondary vertices, we define the two-dimensional decay length L_{xy} in the plane transverse to the beamline, and require its uncertainty δL_{xy} to be less than 0.15 mm. L_{xy} is calculated as $L_{xy} = \frac{\vec{l}_{vtx} \cdot \vec{p}_T^B}{p_T^B}$, where p_T^B is the transverse momentum of the candidate B_s^0, and $\vec{l}_{vtx}$ represents the vector pointing from the primary vertex to the secondary vertex. The uncertainty on the transverse decay length, δL_{xy}, is calculated by taking into account the uncertainties in both the primary and secondary vertex positions. The primary vertex itself is found for each event using a beam-spot constrained fit as described in Ref. [8].

Next, the number of $B_s^0 \to \phi\mu^+\mu^-$ candidates is further reduced by requiring $p_T^B > 5$ GeV/c and asking the B_s^0 candidate vertex to have $\chi^2 < 36$ with 5 d.o.f. The two tracks forming the ϕ candidate are further required to have $p_T > 0.7$ GeV/c and their invariant mass within the range $1.008 < m_\phi < 1.032$ GeV/c^2. The successive cuts and the remaining candidates surviving each cut are shown in Table I.

We apply the same selection for the resonant $B_s^0 \to J/\psi\phi$ candidates except that the invariant mass of the muon pair is now required to be within ± 250 MeV/c^2 of the J/ψ mass.

For the final event selection, we require the candidate events to satisfy additional criteria. The long lifetime of the B_s^0 mesons allows us to reject the random combinatoric background. For this purpose we use the decay length significance $L_{xy}/\delta L_{xy}$ as one of the discriminating variables, since it gives better discriminating power than the transverse decay length alone.

The fragmentation characteristics of the b quark are such that most of its momentum is carried by the B hadron. Thus the number of extra tracks near the B_s^0 candidate tends to be small. Therefore the second discriminant is an isolation variable, $\mathcal{I}$, of the muon and kaon pairs, defined as:

$$\mathcal{I} = \frac{|\vec{p}(\phi\mu^+\mu^-)|}{|\vec{p}(\phi\mu^+\mu^-)| + \sum_{\text{track}\,i \neq B} p_i(\Delta\mathcal{R} < 1)}. \quad (1)$$

Here, $\sum_{\text{track}\,i \neq B} p_i$ is the scalar sum over all tracks excluding the muon and kaon pairs within a cone of $\Delta\mathcal{R} < 1$ around the momentum vector $\vec{p}(\phi\mu^+\mu^-)$ of the B_s^0 candidate where $\Delta\mathcal{R} = \sqrt{(\Delta\phi)^2 + (\Delta\eta)^2}$. The final discriminating variable used is the pointing angle α, defined as the angle between the momentum vector $\vec{p}(\phi\mu^+\mu^-)$ of the B_s^0 candidate and the vector $\vec{l}_{vtx}$ between the primary and secondary vertices. This requirement ensures consistency between the direction of the decay vertex and the momentum vector of the B_s^0 candidate.

We generate signal Monte Carlo (MC) events for the decay $B_s^0 \to \phi\mu^+\mu^-$ using a decay model which includes the NNLO improved Wilson coefficients [9] for the short-distance part. The form factors obtained from QCD light-cone sum rules are taken from Ref. [10]. These form factors were originally determined for $B \to K^*$ transitions and were compared with experimental measurements of the branching fraction $\mathcal{B}(B_d^0 \to K^* \ell^+ \ell^-)$ in Ref. [9]. Recently, new form factors for the $B_s^0 \to \phi$ transition, obtained from the light-cone QCD sum rules, were published [11]. The difference between the form factors in Ref. [9] and those in Ref. [11] reaches 20% for $m_{\mu^+\mu^-} < 1$ GeV/c^2, while elsewhere it remains well below 10%.

The analysis is carried out based on signal MC events in the B_s^0 mass region and on data events in regions outside the experimental signal window defined as $4.51 < m_{\phi\mu^+\mu^-} < 6.13$ GeV/c^2. A 44 MeV/c^2 mass shift in the mass region of interest is introduced to calibrate the D0 tracker.

In order to avoid biasing the analysis procedure, data candidates in the signal mass region are not examined until completion of the analysis, and events in the sideband regions around the B_s^0 mass are used instead. The expected mass resolution for $B_s^0 \to \phi\mu^+\mu^-$ in the MC is 75 MeV/c^2. The start (end) of the upper (lower) sideband was chosen such that it is at least 270 MeV/c^2 away from the B_s^0 mass. The widths of the sidebands used for background estimation are chosen to be 540 MeV/c^2 each. The size of the blind signal region is ± 225 MeV/c^2 which corresponds to a $\pm 3\sigma$ region around the B_s^0 mass. To determine the final limit on the branching fraction, we use a smaller mass region of $\pm 2.5\sigma$.

A random-grid search [12] was used to find simultaneously the optimal values of the discriminants by maximizing the figure of merit [13] $P = \epsilon_{\text{sig}}/(a/2 + \sqrt{N_{\text{back}}})$.
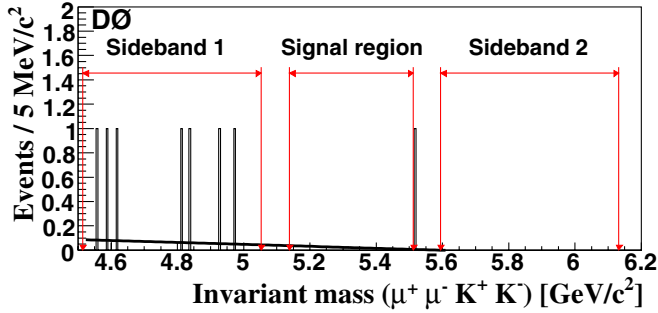
FIG. 1 (color online). The invariant mass distribution after optimized requirements on the discriminating variables. The solid line shows the sidebands background interpolation into the signal region.

FIG. 2. The invariant mass distribution of the normalization channel $B_s^0 \to J/\psi\phi$ after all selection criteria.

Here, ϵ_{sig} is the reconstruction efficiency of the signal events relative to the preselection (estimated using MC), and N_{back} is the expected number of background events interpolated from the sidebands. The constant a is the number of standard deviations corresponding to the confidence level at which the signal hypothesis is tested. This constant a was set to 2.0, corresponding to about the 95% C.L. After optimization, we find the following values for the discriminating variables: $L_{xy}/\delta L_{xy} > 10.3$, $I > 0.72$, and $\alpha < 0.1$ rad.

The total signal efficiency relative to preselection of the three discriminating cuts is $(54 \pm 3)\%$ where the uncertainty is statistical only. After a linear interpolation of the sideband population for the whole data sample into the mass window signal region, we obtain an expected number of 1.6 ± 0.4 background events with statistical uncertainty only.

Upon examining the data in the mass region, zero candidate events are observed in the signal region, consistent with the background events as estimated from sidebands. Figure 1 shows the remaining events populating the lower and upper sidebands. The Poisson probability of observing zero events for an expected background of 1.6 ± 0.4 is $p = 0.22$.

In the absence of an apparent signal, a limit on the branching fraction $\mathcal{B}(B_s^0 \to \phi\mu^+\mu^-)$ can be computed by normalizing the upper limit on the number of events in the B_s^0 signal region to the number of reconstructed $B_s^0 \to J/\psi\phi$ events:

$$\frac{\mathcal{B}(B_s^0 \to \phi\mu^+\mu^-)}{\mathcal{B}(B_s^0 \to J/\psi\phi)} = \frac{N_{\text{ul}}}{N_{B_s^0}} \cdot \frac{\epsilon_{J/\psi\phi}}{\epsilon_{\phi\mu^+\mu^-}} \cdot \mathcal{B}(J/\psi \to \mu^+\mu^-),$$

(2)

where N_{ul} is the upper limit on the number of signal decays, estimated from the number of observed events and expected background events, and $N_{B_s^0}$ is the observed number of $B_s^0 \to J/\psi\phi$ events. The measured branching fractions are $\mathcal{B}(J/\psi \to \mu^+\mu^-) = (5.88 \pm 0.10) \times 10^{-2}$ and $\mathcal{B}(B_s^0 \to J/\psi\phi) = (9.3 \pm 3.3) \times 10^{-4}$ [14]. The global efficiencies of the signal and normalization channels
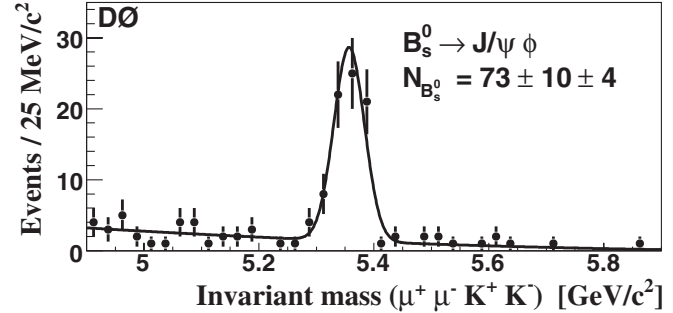
are $\epsilon_{\phi\mu^+\mu^-}$ and $\epsilon_{J/\psi\phi}$ respectively, and include all event selection cuts and the acceptance relative to the entire dimuon mass region. They are determined from MC yielding an efficiency ratio of $(\epsilon_{J/\psi\phi}/\epsilon_{\phi\mu^+\mu^-}) = 2.80 \pm 0.21$, where the uncertainty is due to MC statistics. Applying no cut around the charmonium resonances the efficiency ratio would be $(\epsilon_{J/\psi\phi}/\epsilon'_{\phi\mu^+\mu^-}) = 1.06 \pm 0.07$. In order to avoid large uncertainties associated with the poorly known branching fraction of $B_s^0 \to J/\psi\phi$, we normalize the limit of $B_s^0 \to \phi\mu^+\mu^-$ relative to $\mathcal{B}(B_s^0 \to J/\psi\phi)$ as shown by Eq. (2).

The same cuts are applied to the $B_s^0 \to J/\psi\phi$ candidates. The contamination of muon pairs from the nonresonant $\phi\mu^+\mu^-$ decay in the resonant normalization region $J/\psi(\to \mu^+\mu^-)\phi$ is negligible. We therefore constrain the two muons to have an invariant mass equal to the J/ψ mass [14] when calculating the $\mu^+\mu^-K^+K^-$ invariant mass. The mass spectrum of the reconstructed $B_s^0 \to J/\psi\phi$ is shown in Fig. 2. A fit using a Gaussian function for the signal and a second order polynomial for the background yields $73 \pm 10 \pm 4$ B_s^0 candidates, where the first uncertainty is due to statistics and the second represents the systematic uncertainty which is estimated by varying the fit range as well as the background and signal shape hypotheses.

The different sources of relative uncertainty that enter into the limit calculation of $\mathcal{B}$ of $B_s^0 \to \phi\mu^+\mu^-$ are given in Table II. The largest uncertainty, 25%, is due to the background interpolation into the signal region and is based on the statistical uncertainty of the fit integral. The uncertainty on the number of observed $B_s^0 \to J/\psi\phi$ events in the normalization channel is 14.8%.

The p_T distribution of the B_s^0 in data is on average slightly higher than that from MC. Therefore, MC events for the signal and normalization channels have been reweighted accordingly and an additional uncertainty of 3.7% is applied. The *CP*-even signal MC events are generated with a B_s^0 lifetime of 1.44 ps [15]. To account for a possible efficiency difference related with the shorter lifetime of the *CP*-even B_s^0, the signal MC events are weighted according to the combined world average *CP*-even lifetime [16]. The efficiency difference is estimated to be 8% which

TABLE II. The relative uncertainties found for the upper limit on $\mathcal{B}$.

Source	Relative Uncertainty [%]
# of $B_s^0 \to J/\psi\phi$	14.8
$\epsilon_{J/\psi\phi}/\epsilon_{\phi\mu\mu}$	7.5
MC weighting	3.7
CP-even lifetime	8.0
$\mathcal{B}(J/\psi \to \mu\mu)$	1.7
Total	18.9
Background uncertainty	25.0

is taken as an additional systematic uncertainty. The statistical uncertainty on the efficiency ratio $\epsilon_{J/\psi\phi}/\epsilon_{\phi\mu^+\mu^-}$ is found to be 7.5%. The signal efficiency obtained from MC is based on the input for the NNLO Wilson coefficients and form factors of Ref. [9]. We do not include any theoretical uncertainty in our systematics uncertainty estimation. The statistical and systematic uncertainties can be included in the limit calculation by integrating over probability functions that parameterize the uncertainties. We use a prescription [17] where we construct a frequentist confidence interval with the Feldman and Cousins [18] ordering scheme for the MC integration. The background is modeled as a Gaussian distribution with its mean value equal to the expected number of background events and its standard deviation equal to the background uncertainty. Including the statistical and systematic uncertainties, the Feldman and Cousins (FC) limit is

$$\frac{\mathcal{B}(B_s^0 \to \phi\mu^+\mu^-)}{\mathcal{B}(B_s^0 \to J/\psi\phi)} < 4.4(3.5) \times 10^{-3}$$

at the 95% (90%) C.L. respectively [19]. Taking a

Bayesian approach [20] with a flat prior and the uncertainties treated as Gaussian distributions in the integration, we find an upper limit of $\mathcal{B}(B_s^0 \to \phi\mu^+\mu^-)/\mathcal{B}(B_s^0 \to J/\psi\phi) < 7.4(5.6) \times 10^{-3}$ at the 95% (90%) C.L., respectively.

Since we have fewer events observed than expected, we also quote the sensitivity of our search. Assuming there is only background, we calculate for each possible value of observation a 95% C.L. upper limit weighted by the Poisson probability of occurrence. Including the statistical and systematical uncertainties, our sensitivity is given by $\langle\mathcal{B}(B_s^0 \to \phi\mu^+\mu^-)\rangle/\mathcal{B}(B_s^0 \to J/\psi\phi) = 1.1(1.2) \times 10^{-2}$ at the 95% C.L. using the FC (Bayesian) approaches, respectively.

Using only the central value of the world average branching fraction [14] of $\mathcal{B}(B_s^0 \to J/\psi\phi) = (9.3 \pm 3.3) \times 10^{-4}$, the FC limit corresponds to $\mathcal{B}(B_s^0 \to \phi\mu^+\mu^-) < 4.1(3.2) \times 10^{-6}$ at the 95% (90%) C.L. respectively. This is presently the most stringent upper bound and can be compared with the SM calculation of $\mathcal{B}(B_s^0 \to \phi\mu^+\mu^-) = 1.6 \times 10^{-6}$ of Ref. [3].

[1] B. Aubert *et al.* (*BABAR* Collaboration), hep-ex/0507005.
[2] A. Ishikawa *et al.* (Belle Collaboration), Phys. Rev. Lett. **91**, 261601 (2003).
[3] C. Q. Geng and C. C. Liu, J. Phys. G **29**, 1103 (2003).
[4] A. Deandrea and A. Polosa, Phys. Rev. D **64**, 074012 (2001).
[5] D. Acosta *et al.* (CDF Collaboration), Phys. Rev. D **65**, 111101 (2002).
[6] V. M. Abazov *et al.* (D0 Collaboration), physics/0507191.
[7] V. M. Abazov *et al.* (D0 Collaboration), Phys. Rev. Lett. **94**, 232001 (2005).
[8] J. Abdallah *et al.* (DELPHI Collaboration), Eur. Phys. J. C **32**, 185 (2004).
[9] A. Ali *et al.*, Phys. Rev. D **66**, 034002 (2002).
[10] A. Ali *et al.*, Phys. Rev. D **61**, 074024 (2000).
[11] P. Ball and R. Zwicky, Phys. Rev. D **71**, 014029 (2005).
[12] N. Amos *et al.* in *Proc. of Computing in High Energy Physics (CHEP'95)*, edited by R. Shellard and T. Nguyen (World Scientific, River Edge, NJ, 1996), p. 215.
[13] G. Punzi, in *Proc. of the Conference on Statistical Problems in Particle Physics, Astrophysics and Cosmology (Phystat 2003)*, edited by L. Lyons *et al.* (SLAC, Menlo Park, CA, 2003), p. 79.
[14] S. Eidelman *et al.*, Phys. Lett. B **592**, 1 (2004).
[15] V. M. Abazov *et al.* (D0 Collaboration), Phys. Rev. Lett. **94**, 042001 (2005).
[16] Heavy Flavor Averagaing Group (HFAG), hep-ex/0505100.
[17] J. Conrad *et al.*, Phys. Rev. D **67**, 012002 (2003).

[18] G. J. Feldman and R. D. Cousins, Phys. Rev. D **57**, 3873 (1998).

[19] This limit is obtained for the full phase space, i.e., interpolating into the mass region of the charmonium resonances. Using only the actual selected dimuon mass region a limit (FC) of $\frac{\mathcal{B}(B_s^0 \to \phi\mu^+\mu^-)}{\mathcal{B}(B_s^0 \to J/\psi\phi)} < 1.7(1.3) \times 10^{-3}$ is obtained at the 95% (90%) C.L. by replacing $(\epsilon_{J/\psi\phi}/\epsilon_{\phi\mu^+\mu^-}) =$

2.80 ± 0.21 with $(\epsilon_{J/\psi\phi}/\epsilon'_{\phi\mu^+\mu^-}) = 1.06 \pm 0.07$ of Eq. (2). We have also estimated the relative efficiency ratio of normalization to signal channel for the full dimuon mass region with a second form factor calculation from Ref. [11] and obtained $(\epsilon_{J/\psi\phi}/\epsilon'_{\phi\mu^+\mu^-}) = 1.04 \pm 0.07$.

[20] I. Bertram *et al.*, Fermilab Report No. Fermilab-TN-2401 (unpublished).